
BiMarker: Enhancing Text Watermark Detection for Large Language Models with Bipolar Watermarks

Zhuang Li^{* 1}

Abstract

The rapid proliferation of Large Language Models (LLMs) has raised concerns about misuse and the challenges of distinguishing AI-generated text from human-written content. Existing watermarking techniques, such as KGW, still face limitations under low watermark strength, stringent false-positive requirements, and low-entropy scenarios. Our analysis reveals that current detection methods rely on coarse estimates of non-watermarked text, which constrains watermark detectability. We propose the Bipolar Watermark (BiMarker), a novel approach that divides generated text into positive and negative poles, leveraging the difference in green token counts for detection. This differential mechanism significantly enhances the detectability of watermarked text. Theoretical analysis and experimental results demonstrate BiMarker’s effectiveness and compatibility with existing optimization techniques, providing a new dimension for watermarking in LLM-generated content.

1. Introduction

In recent years, Large Language Models (LLMs) have revolutionized natural language processing (OpenAI, 2022; Touvron et al., 2023; Bubeck et al., 2023), but their widespread adoption has also raised significant concerns. These models can be exploited for malicious purposes, such as generating fake news, fabricating academic papers, and manipulating public opinion through social engineering and disinformation campaigns (Bergman et al., 2022; Jawahar et al., 2020). Additionally, the proliferation of synthetic data on the web complicates dataset curation, as it often lacks the quality of human-generated content and must be carefully filtered during training (Radford et al., 2023). As a result, developing effective methods to reliably distinguish AI-generated text from human-written content has become a critical and

urgent priority (Bender et al., 2021; Crothers et al., 2022; Grinbaum & Adomaitis, 2022; Wyllie et al., 2024).

Watermarking techniques offer a solution by enabling LLMs to embed unique, imperceptible identifiers (watermarks) within generated content, distinguishing it from human-written text. A prominent method, KGW¹, achieves high detection performance with low false positive and false negative rates (Kirchenbauer et al., 2023a). KGW works by partitioning the model’s vocabulary into two categories: *green* and *red* tokens, with proportions γ and $1 - \gamma$, respectively. The model is then biased towards green tokens by adjusting their logits with a positive constant (watermark strength), ensuring that the generated text predominantly contains green tokens. During detection, KGW assumes that the number of green tokens in non-watermarked text follows a Gaussian distribution $\mathcal{N}(\mu, \sigma^2)$, where $\mu = T \cdot \gamma$ and $\sigma^2 = T \cdot \gamma \cdot (1 - \gamma)$, with T representing the number of tokens analyzed. The likelihood that the text is watermarked increases as the observed number of green tokens deviates from the expected $T \cdot \gamma$. In other words, the greater the number of green tokens in the analyzed text exceeds the expected value of $T \cdot \gamma$ for non-watermarked text, the higher the probability that the text is watermarked.

Although KGW demonstrated high detection performance, it exhibited weaknesses under more rigorous detection conditions, particularly in low-entropy scenarios (Lee et al., 2024). Furthermore, it is crucial for detection methods to effectively distinguish between human-written and watermarked text to achieve higher accuracy while minimizing false positives, as false positives are intolerable in many contexts (Fernandez et al., 2023; Lee et al., 2024; Kirchenbauer et al., 2023b), such as falsely accusing a user of producing fake news or a student of cheating in an exam. A straightforward strategy is to increase watermark strength, which can help address this issue by enhancing the distinguishability between watermarked and non-watermarked texts. However, this improvement often comes at the cost of text quality (Tu et al., 2023).

Recent studies have proposed algorithms aimed at enhancing the statistical significance of detected watermarked text

¹School of Computer Science, Beijing University of Posts and Telecommunications, Beijing, China. Correspondence to: Zhuang Li <bupt01@bupt.edu.cn>.

¹Details can be found in Appendix A.2

by leveraging its relationship with entropy (Lee et al., 2024; Lu et al., 2024). For example, Lee et al. (2024) introduced a selective watermark detector called SWEET, specifically designed for code generation tasks, to improve watermark detectability in code. This method detects only those tokens that exceed a certain entropy threshold, thereby excluding tokens less likely to be influenced by the watermark generator. However, these algorithms depend on an auxiliary language model for vocabulary partitioning, which proves impractical when the tokenizers of the primary and auxiliary models are inconsistent (Yoo et al., 2024). Moreover, retrieving entropy values during detection necessitates access to the prompt’s content. While the effectiveness of custom prompts has been demonstrated in code-related tasks (Lee et al., 2024; Lu et al., 2024), applying this approach to general tasks poses significant challenges.

Orthogonal to prior work, this paper proposes a novel perspective for enhancing the distinction between watermarked and non-watermarked texts. Our approach is based on the analysis that existing methods often overlook the impact of non-watermarked text distributions across different scenarios on detection outcomes (see Section 3.1). Specifically, taking KGW as an example, the held assumption that the number of green tokens in non-watermarked text has an expected value of $T \cdot \gamma$ does not consistently hold across various contexts. In some cases, this assumption undermines detection effectiveness². For example, in low-entropy scenarios, both watermarked and non-watermarked texts tend to have a similarly small expected number of green tokens. Continuing to assume this fixed value as the expected value for non-watermarked text results in a lack of statistical significance, thereby increasing the risk of failing to effectively distinguish between watermarked and non-watermarked text.

To address the challenges posed by inaccurate green token count estimations in non-watermarked text that affect detection results, we propose *Bipolar WaterMarker* (abbreviated as **BiMarker**). As illustrated in Figure 1, the generated text is divided into two components: the *positive pole* and the *negative pole*. In the positive pole, the logits of tokens in the green list are increased by adding a positive constant, while in the negative pole, the logits of tokens in the red list are adjusted similarly. For detection, instead of comparing the number of green tokens to the ideal expected count, we calculate the green token counts in both poles and determine their difference. This approach significantly enhances the distinction between watermarked and human-written text. Moreover, through various analyses, we demonstrate that our method is orthogonal to existing techniques that leverage entropy or enhance watermark detection. It can be

²Appendix A.3 provides an example illustrating the detection challenges arising from inaccurate estimations of non-watermarked text.

effectively combined with these optimization techniques in scenarios where entropy can be computed and prompts are available.

In summary, the key contributions of our work are summarized as follows:

- **New Dimension:** We reveal the impact of inaccurate estimations of human-written text distributions on detection results, offering a new perspective for enhancing the detectability of watermarks.
- **New Method:** We introduce **BiMarker**, a novel bipolar watermarking method with differential detection. This approach effectively addresses the challenges posed by the estimation inaccuracies of human-written text distributions, enhancing the distinction between watermarked and human-generated content.
- **Theoretical Proof:** We provide a comprehensive theoretical analysis of detection accuracy, demonstrating that our method improves the detectability of watermarked text without increasing the false positive rate, and that it is equally effective when used in conjunction with other optimization techniques.
- **Experimental Validation:** Our experiments demonstrate that **BiMarker** surpasses traditional watermarking methods in detection accuracy. Additionally, it is fully compatible with entropy-based watermark optimization techniques.

2. Related Works

Text watermarking is a form of linguistic steganography, where the objective is to embed a hidden message—the watermark—within a piece of text. Typically, text watermarking is divided into two main categories: watermarking for existing texts and watermarking for Large Language Models (LLMs).

2.1. Watermarking for Existing Texts

Some methods embed watermarks by modifying the text format rather than its content, such as line or word-shift coding or Unicode modifications like whitespace replacement (**WhiteMark**) and variation selectors (**VariantMark**) (Brassil et al., 1995; Sato et al., 2023). While these approaches preserve the meaning of the text and allow for high payloads, they are vulnerable to removal through canonicalization (e.g., resetting spacing) (Por et al., 2012) and can be easily forged, which compromises their reliability (Boucher et al., 2022).

Some watermarking methods modify the content of the text, such as by changing words (Topkara et al., 2006; Fellbaum,

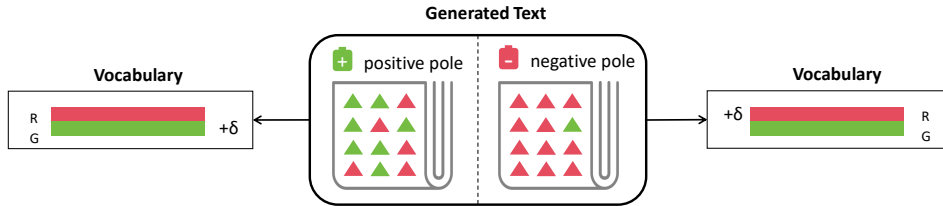


Figure 1. Bipolar Watermark.

1998; Munyer & Zhong, 2023; Yang et al., 2022; 2023). Yang et al.(Yang et al., 2022) introduced a BERT-based in-fill model to generate contextually appropriate lexical substitutions, along with a watermark detection algorithm that identifies watermark-bearing words and applies inverse rules to extract the hidden message. In another work, Yang et al.(Yang et al., 2023) simplified detection by encoding words with random binary values, substituting bit-0 words with context-based synonyms for bit-1. However, these lexical substitution methods can be vulnerable to simple removal techniques, such as random synonym replacement.

2.2. Watermarking for LLMs

Watermark embedding during LLM generation can be achieved by modifying token sampling (Kuditipudi et al., 2023; Christ et al., 2023b) or model logits (Kirchenbauer et al., 2023a; Yoo et al., 2024; Ren et al., 2024; Lu et al., 2024), resulting in more natural text. KGW (Kirchenbauer et al., 2023a) represents a promising approach for distinguishing language model outputs from human text while maintaining robustness against realistic attacks, as it can reinforce the watermark with every token. Several studies have built upon KGW, addressing various aspects such as low-entropy generation tasks like code generation (Lee et al., 2024; Lu et al., 2024), enhancing watermark undetectability (Christ et al., 2023a), enhancing performance in payload (Yoo et al., 2024; Wang et al., 2023) and improving robustness (Munyer & Zhong, 2023; Zhao et al., 2023; Liu et al., 2024; Ren et al., 2024). For example, Fernandez et al. (2023) expanded from a binary red-green partition to a multi-color partition through fine-grained vocabulary partitioning, allowing for the embedding of multi-bit watermarks. Additionally, Ren et al. (2024) converted semantic embeddings into semantic values using weighted embedding pooling, followed by discretization with NE-Ring, and classified the vocabulary into red-list and green-list categories based on these semantic values, thus enhancing robustness.

Some existing methods aim to improve the detectability of KGW in low-entropy scenarios (Lu et al., 2024; Lee et al., 2024). For instance, Lu et al. (2024) addresses this by assigning weights to tokens based on their entropy during detection, thereby enhancing sensitivity by emphasizing high-entropy tokens in z-score calculations. In contrast,

our approach does not require using large language models to compute token entropy during detection, nor does it depend on the availability of prompt content. Moreover, our method is orthogonal to these approaches, allowing it to be seamlessly integrated with such techniques for enhanced performance.

3. Method

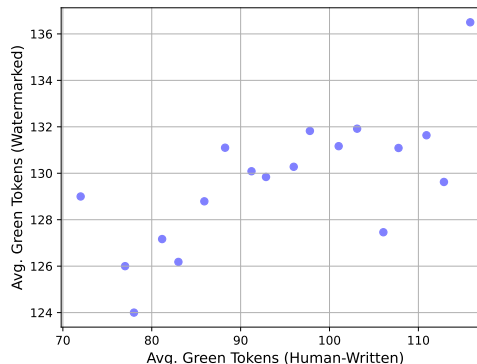


Figure 2. Empirical Study of the Relationship Between the Number of Green Tokens in Human-Written Texts and the Number of Green Tokens in Watermarked Texts.

3.1. Motivation

Before presenting our method, we first outline a key assumption: *the process of human-written text generation and machine-generated text generation are similar*. Specifically, we assume that the process by which a LLM generates text without watermarking can be considered analogous to the process of human text writing. This assumption is grounded in the design of LLMs, which are trained on extensive datasets of human-written text to learn patterns, structures, and styles. As a result, their outputs often demonstrate fluency, coherence, and stylistic consistency that closely resemble human-written text, making this analogy plausible. Thus, by substituting human-written text into (7) with $\alpha = 1$, we obtain: $\mathbb{E}|s|_G \geq \frac{\gamma T}{1+(\alpha-1)\gamma} S^* = \gamma T S^*$, Where S^* represents the theoretical lower bound. This indicates that the number of green tokens in human-written text is also related to entropy, with the average number of green

tokens tending to be lower when entropy is low. Therefore, we believe that during the detection of watermarked text, a lower average number of green tokens suggests a corresponding decrease in the average number of green tokens in human-written text.

We conducted a simple empirical study, assuming that 200 tokens are generated using the KGW watermarking algorithm ($\gamma = 0.5$ and $\delta = 1$, employing polynomial sampling) with OPT-1.3B (Zhang et al., 2022) and prompts sourced from the RealNewsLike subset of the C4 dataset (Raffel et al., 2020) across approximately 500 generations. We detect the number of green tokens in both human-written and watermarked texts. We select the portion of human-written text where the number of green tokens is less than 120, dividing the data into intervals of 2.5 based on the number of green tokens. Then, we calculate the average number of green tokens in human-written text and the corresponding watermarked text for each interval. The relationship between the number of green tokens in watermarked texts and those in human-written texts is analyzed, with the results visualized in Figure 2. From the figure, we observe that when the number of green tokens in human-written text is low, the number of green tokens in watermarked text also tends to be smaller. We calculate their Pearson correlation coefficient, which is 0.700. This demonstrates a strong positive relationship, suggesting that lower green token counts in human-written text are more likely to correspond to lower counts in watermarked text.

However, KGW only consider the theoretical lower bound of green tokens in watermarked texts under varying entropy conditions, overlooking the fact that the expected number of green tokens in non-watermarked texts also varies with entropy. During detection, these methods continue to rely on the difference between the number of green tokens in the analyzed text and the expected fixed value; a larger difference indicates stronger statistical significance. However, this approach is clearly insufficient.

To correct the existing algorithms’ inaccurate estimation of the number of green tokens in human-written texts and its impact on detection results, one intuitive solution would be to utilize a non-watermarked LLM during detection to approximate the number of green tokens in the output text. However, we did not pursue this approach because it would introduce additional inference costs, and in many cases, the prompt itself may not be available. Our goal is to develop an algorithm that does not increase time complexity and can be applied in any scenario.

3.2. Our Method

Generating the Watermark. Our watermark embedding algorithm, as outlined in Algorithm 1, differs from the KGW algorithm, which uniformly boosts the scores of green to-

Algorithm 1 Text Generation with Bipolar Watermarks

Input: prompt x_{prompt} , $\gamma \in (0, 1)$, $\delta > 0$, $\rho \in (0, 1)$

for $i = 0, 1, 2, \dots$ **do**

Compute a logit vector l_i by (2);

Compute a hash of token $s_{:i}$, and use it to seed a random number generator;

Using this random number generator, randomly partition the vocabulary into two lists, $list1$ and $list2$, with sizes $\gamma|V|$ and $(1 - \gamma)|V|$, respectively;

Use the generator to decide the current polarity p (positive or negative) according to the probability ρ ;

if p is positive **then**

$list1$ is the green token list G , and $list2$ is the red token list R ;

Add δ to the logits of tokens in G ;

else

$list2$ is the green token list G , and $list1$ is the red token list R ;

Add δ to the logits of tokens in R ;

end if

Sample s_i by (3);

end for

kens across all generated text. Instead, our approach divides the generated text into positive and negative polarities. In the positive polarity phase, the algorithm increases the logits of tokens in the green list to enhance their sampling probabilities. Conversely, in the negative polarity phase, it increases the logits of tokens in the red list, thereby reducing the sampling probabilities of green tokens. The polarity (positive or negative) is pseudo-randomly determined based on the probability ρ , where ρ represents the probability of the positive polarity. This approach avoids hardcoding the polarities into the input text sequence, thereby reducing the risk of detection failure caused by confusion in non-watermarked text scenarios. Notably, our method consistently increases logits across γ proportion of the vocabulary, resulting in a distribution change for the generated text that is consistent with KGW. Notably, our method consistently increases logits across a γ proportion of the vocabulary, resulting in an overall distribution change for the generated text that aligns with KGW. This implies that under identical γ and δ , our method maintains the same variations in text quality as KGW (see Appendix A.2).

Detecting the watermark. We can detect the watermark by testing the following null hypothesis H_0 : *The text sequence is generated without any knowledge of the red list rule or the polarity rule.*

During detection, we count the number of positive and negative green tokens, denoted as $|s|_{pG}$ and $|s|_{nG}$, respectively. Let T_p and T_n represent the total numbers of positive and

negative tokens. Under the null hypothesis (H_0), when the distributions of the positive and negative poles are independent, the expected value of $|s|_{pG} - |s|_{nG}$ is $T_p \cdot \gamma - T_n \cdot (1 - \gamma)$, with a variance of $T \cdot \gamma \cdot (1 - \gamma)$, where $T = T_p + T_n$. The z -statistic for this test is calculated as:

$$z = \frac{|s|_{pG} - |s|_{nG} - \gamma T_p + (1 - \gamma) T_n}{\sqrt{T \gamma (1 - \gamma)}}. \quad (1)$$

Remark. From Formula 9, we observe that our numerator still relies on the estimated expectation for the number of green tokens in non-watermarked text. However, this influence is mitigated due to the subtraction of the estimated values for positive and negative polarities. When the number of text sequences generated for the positive and negative polarities satisfies the ratio $T_p/T_n = (1 - \gamma)/\gamma$, the z -value simplifies to:

$$z = \frac{|s|_{pG} - |s|_{nG}}{\sqrt{T \cdot \gamma (1 - \gamma)}}.$$

In this scenario, the z -value directly reflects the observed difference between the counts of positive and negative green tokens. This reduces the reliance on estimated values for non-watermarked text, thereby diminishing the impact of potential inaccuracies in these estimations on the final detection result.

3.3. Effect of Bipolar Watermark

This section demonstrates that our BiMarker improves detectability. Theorem 3.1 indicates that a higher lower bound of the z -score can be achieved using BiMarker compared to KGW. This improvement is realized by reducing the decline in detection accuracy caused by inaccurate estimations of non-watermarked text.

Theorem 3.1. *Consider watermarked text sequences s of T tokens. Each sequence is produced by sequentially sampling a raw probability vector $p(t)$ from the language model, sampling a random green list of size $\gamma|V|$. The sequence s is composed of a positive part s_p and a negative part s_n . The logits for the green and red lists are boosted by δ before sampling each token in the positive and negative parts, respectively. Define $\alpha = \exp(\delta)$, and let $|s|_d$ denote the difference in the number of green list tokens in the positive and negative parts of sequence s . We assume that positive and negative tokens are mutually independent, then BiMarker achieves a theoretical lower bound for the z -score that consistently exceeds that of KGW.*

Furthermore, we present the following theorem regarding non-watermarked text: our differential detection method does not increase the false positive rate.

Theorem 3.2. *For non-watermarked text, we assume that the total number of green tokens follows a Gaussian distribution, $\mathcal{N}(\mu_T, \sigma_T^2)$. Similarly, the numbers of tokens in the positive and negative polarities are assumed to follow Gaussian distributions, $\mathcal{N}(\mu_{T_p}, \sigma_{T_p}^2)$ and $\mathcal{N}(\mu_{T_n}, \sigma_{T_n}^2)$, respectively. Moreover, these two distributions are considered independent of each other.*

We denote the false positive rate generated by the unipolar detection method as F_{KGW} and the false positive rate generated by the differential detection method as F_{DIFF} . Then, we can express the relationship as follows:

$$F_{KGW} \geq F_{DIFF}.$$

The detailed proofs of Theorems 3.1 and 3.2 are provided in Appendix C.

Applying BiMarker to SWEET and EWD. SWEET and EWD are advanced algorithms derived from KGW, designed to enhance the statistical significance of watermark text by leveraging entropy. Our proposed algorithm is orthogonal to both of these approaches. The application of our bipolar watermarking and differential detection algorithms, based on SWEET and EWD, is detailed in Appendix B. Moreover, the conclusions of Theorem 3.1 and Theorem 3.2 remain valid when our algorithms are applied to SWEET and EWD. In other words, our algorithm enhances the statistical significance of watermark text in both SWEET and EWD while preserving the original false positive rate. Below, we elaborate on the effectiveness of applying the bipolar watermarking and differential detection algorithms to SWEET, while the rationale for their application to EWD is explained in Appendix B.

The primary distinction between SWEET and KGW lies in the fact that SWEET applies a bias δ to the logits of tokens in G only if their entropy exceeds a specified threshold τ . This mechanism enables the algorithm to selectively target subsequences of the generated text based on their entropy levels. According to Theorem 3.1 and Theorem 3.2, when such subsequences satisfy the conditions outlined in our theoretical framework, the following conclusions can be drawn: applying SWEET with our bipolar watermarking and differential detection algorithms results in higher theoretical lower bounds for the z -values, without increasing the false positive rate.

4. Experiments

In this section, we first evaluate the performance of BiMarker and KGW under high-entropy conditions to demonstrate the effectiveness of our watermarking algorithm. Subsequently, we assess the performance of BiMarker when used in conjunction with existing KGW-based optimization

algorithms, SWEET and EWD, in code-related tasks, which are their primary focus. This evaluation illustrates that our algorithm is orthogonal to other optimization methods, providing new insights for future optimization approaches.

To assess the performance of the watermark, we primarily analyze the True Positive Rate (TPR) and False Positive Rate (FPR), where TPR represents the detection of watermarked text, and FPR indicates human text falsely flagged as watermarked. We also present the F1 score as an additional metric. Our implementation is based on the completion of KGW with the probability ratio of positive and negative polarities set to $(1 - \gamma)/\gamma$.

Tasks and Datasets. Our experiments are designed with two scenarios. The first scenario is a high-entropy environment, where we use the same experimental dataset as KGW and employ the OPT-1.3B (Zhang et al., 2022) model to generate watermarked texts. To simulate diverse and realistic language modeling conditions, we randomly select texts from the news-like subset of the C4 dataset (Raffel et al., 2020). Following KGW’s setup, for each randomly selected string, a fixed number of tokens are trimmed from the end to serve as the baseline completion, with the remaining tokens acting as the prompt. In all experiments, we generate 500 samples, each with a length of approximately 200 ± 5 tokens.

The second scenario focuses on low-entropy conditions, which are the primary target of SWEET and EWD. For this, we adopt the task of code generation, using two datasets: HumanEval (Chen et al., 2021) and MBPP (Austin et al., 2021), following Lee et al. (2024). These datasets consist of Python programming problems with test cases and corresponding reference answers, which are treated as human-written samples. Code generation is conducted using StarCoder (Li et al., 2023). During evaluation, the length of both the generated and reference samples is restricted to at least 15 tokens. For more detailed experimental settings, please refer to Appendix D.1.

Main Results. Figure 3 illustrates the relationship between watermark strength (represented by δ) and accuracy under various hyperparameter settings. Additional metrics, including ROC curves, are provided in Appendix D.2. We consider combinations of $\gamma = [0.25, 0.5]$ and $\delta = [0.25, 0.75, 1, 1.5, 2, 2.5]$, utilizing both multinomial sampling and 8-beam search. It is clear that larger δ values result in stronger watermarking, but at the cost of text quality. Given that incorrectly labeling human-written texts as watermarked carries more significant consequences than falsely identifying watermarked texts as human-written (Fernandez et al., 2023; Lee et al., 2024; Kirchenbauer et al., 2023b), we focus on the accuracy in scenarios where no false positives (0/500) are observed.

Table 1. TPR at various FPR for watermark detection using KGW and BiMarker are presented, with $\gamma = 0.5$. The first three comparisons employ multinomial sampling, while the final comparison utilizes beam search with a beam size of 8.

METHODS	δ	1%FPR		5%FPR	
		TPR	F1	TPR	F1
KGW	0.5	0.436	0.603	0.7	0.8
BiMARKER	0.5	0.498	0.66	0.744	0.829
KGW	1.5	0.978	0.984	0.992	0.972
BiMARKER	1.5	0.986	0.988	0.992	0.972
KGW	2.0	0.99	0.99	0.994	0.973
BiMARKER	2.0	0.994	0.992	0.994	0.973
KGW	2.0	0.998	0.994	1.0	0.976
BiMARKER	2.0	0.998	0.994	1.0	0.976

From the figure, we observe that BiMarker outperforms KGW in distinguishing watermarked texts from human-written texts, particularly when the watermarking strength is low. The enhancement in performance is more pronounced under multinomial sampling compared to 8-beam search. Notably, under multinomial sampling, when δ is set to 1, the TPR increases by 10% with no false positives, and at $\delta = 0.75$, it can even increase by 20%. In contrast, when δ is set to 2.5 under 8-beam search, both methods achieve a TPR of 1. Table 1 presents the accuracy and F1 scores under TPR at 1% and 5% false positive rates for different watermark strengths when $\gamma = 0.5$. The observed trends are consistent with those in Figure 3. These results demonstrate the effectiveness of BiMarker across various hyperparameter settings.

Analysis of the Reasons for Performance Improvement.

Figure 4 shows the z-scores of both watermarked and human texts under different hyperparameter settings, detected by various methods. Our BiMarker method results in overall higher z-scores for watermarked texts, while the z-scores for human texts remain relatively unchanged. By enlarging the gap between the z-scores of watermarked and human texts, our BiMarker demonstrates an enhanced ability to distinguish watermarked texts effectively. Furthermore, these results support the validity of our Theorem 3.1 and Theorem 3.2.

Performance with Different Numbers of Tokens. Figure 5 shows the detected average z-score over samples as T varies. The curves are presented for various values of δ and γ using multinomial sampling. We observe that, compared to KGW, BiMarker does not sacrifice its detection capability on short text sequences. BiMarker consistently achieves higher z-scores for watermarked texts across different values of T compared to KGW.

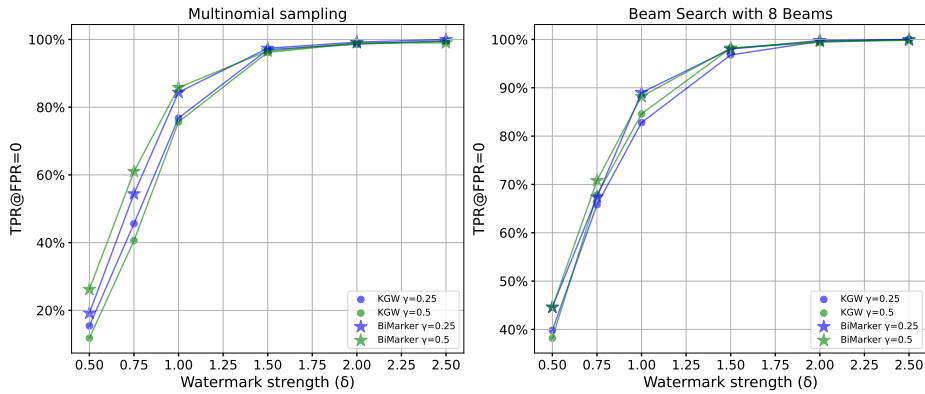


Figure 3. The relationship between watermark strength and accuracy under zero false positives (0/500). The left figure illustrates results with multinomial sampling, while the right figure depicts results using beam search with a beam size of 8.

Table 2. Comparison of Detection Results Before and After Applying the BiMarker Algorithm to KGW, SWEET and EWD Across Different Datasets ($\gamma = 0.5, \delta = 2$)

METHODS	HUMANEVAL					MBPP				
	1%FPR		5%FPR		BEST	1%FPR		5%FPR		BEST
	TPR	F1	TPR	F1	F1	TPR	F1	TPR	F1	F1
KGW	0.375	0.542	0.5	0.645	0.787	0.098	0.177	0.347	0.497	0.739
KGW+BiMARKER	0.352	0.516	0.609	0.734	0.797	0.176	0.296	0.38	0.531	0.749
SWEET	0.561	0.714	0.758	0.838	0.875	0.381	0.548	0.686	0.791	0.85
SWEET+BiMARKER	0.563	0.715	0.758	0.838	0.872	0.415	0.582	0.67	0.779	0.852
EWD	0.609	0.753	0.75	0.833	0.869	0.6	0.746	0.762	0.841	0.888
EWD+BiMARKER	0.671	0.799	0.75	0.833	0.96	0.618	0.759	0.833	0.844	0.898

Table 3. Detection performance of back-translated watermarked texts using different watermarking algorithms, with $\gamma = 0.5$.

METHODS	δ	DETECTION W/ BACK-TRANSLATION			
		1%FPR		5%FPR	
		TPR	F1	TPR	F1
KGW	0.5	0.188	0.314	0.488	0.635
BiMARKER	0.5	0.272	0.424	0.496	0.642
KGW	1.5	0.786	0.875	0.914	0.931
BiMARKER	1.5	0.776	0.868	0.93	0.939

Performance against the Back-translation Attack. Watermarked texts are often edited before detection, which can partially remove the watermark and degrade detection performance. To evaluate the robustness of our BiMarker under these conditions, we simulate this scenario by employing back-translation as an attack strategy to alter the watermarked text. Specifically, we first generate watermarked texts and then translate them from English to French before translating them back to English for detection. This approach not only mirrors realistic adversarial scenarios but also ensures that the modifications aim to obscure the

watermark while preserving the semantic integrity of the original text. Table 3 presents our detection results with back-translation. Our experiments show that BiMarker achieves overall better detection accuracy and demonstrates performance comparable to KGW.

Impact of ρ on Results. In Section 3.2, we established that watermark detection performance is maximized when $T_p/T_n = (1 - \gamma)/\gamma$. To verify this conclusion, we conducted experiments. By setting $\gamma = 0.25$ and 0.5 , the theoretically optimal ρ , representing the positive ratio, is 0.75 and 0.5 , respectively. We varied ρ values to compare detection accuracy. To minimize the impact of randomness, we adopted a position-based hard-coded division: the first $200 \cdot \rho$ tokens were assigned to the positive polarity, while the remaining tokens were assigned to the negative polarity. The experimental results, shown in Figure 6, confirm our theoretical prediction, validating the correctness of our theory.

Application of BiMarker to SWEET and EWD. Embedding watermarks in low-entropy texts presents a significant challenge. We evaluate whether our bipolar watermarking

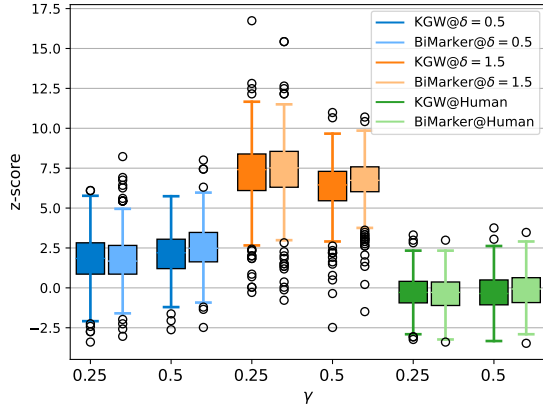


Figure 4. Z-scores of Watermarked and Human Texts under Different Parameter Settings. We set the sampling method to multinomial sampling.

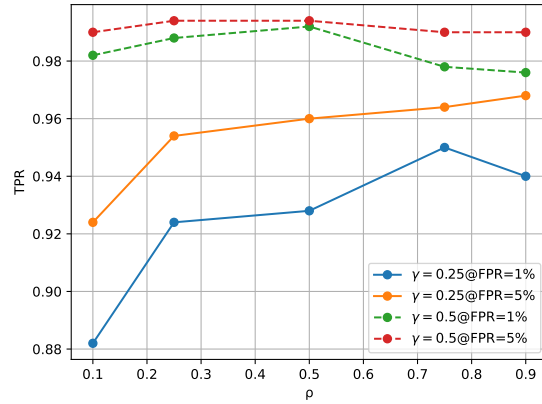


Figure 6. The impact of ρ values on detection results. We set $\delta = 1.5$ and used multinomial sampling.

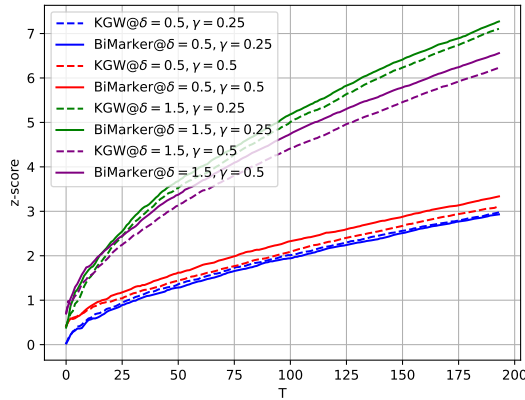


Figure 5. The Average Z-Score as a Function of Token Length (T) of the Generated Text. Different combinations of hyperparameters were used, and the sampling method was set to multinomial sampling.

and differential detection methods can be applied to existing algorithms, including KGW and its variants, SWEET and EWD, with the goal of enhancing their performance and paving the way for future research directions. Specifically, when applied to KGW and EWD, we employ position-based hard encoding for the polarities, using a repeating cycle of 20 positive tokens followed by 20 negative tokens. However, for SWEET, which applies watermark embedding and detection only to high-entropy segments, we select a smaller cycle of 15 positive tokens followed by 15 negative tokens. Table 2 presents the results before and after the application of BiMarker, showing a significant improvement in detection effectiveness. For instance, when applied to the current state-of-the-art algorithm EWD, our BiMarker demonstrates enhancements across all metrics for each dataset.

5. Conclusion

In this work, we reveal the impact of the inaccurate estimation of the number of green tokens in non-watermarked texts by existing watermarking algorithms on watermark detection accuracy. To address this issue, we propose a bipolar watermarking and differential detection algorithm called BiMarker. Instead of comparing the number of green tokens to a fixed value, BiMarker calculates the green token counts in both poles and determines their difference. We conduct both theoretical and experimental analyses to evaluate the effectiveness of BiMarker. The results demonstrate that this algorithm effectively enhances the detectability of watermarks, exhibiting excellent performance, particularly under low watermark strength and low false positive rate conditions. Furthermore, we provide theoretical and experimental evidence showing that our algorithm is orthogonal to SWEET and EWD indicating that its application can significantly improve the detectability of low-entropy texts when integrated with these algorithms. This opens up new avenues for future optimization efforts.

Limitations

Currently, when applying BiMarker with SWEET and EWD in low-entropy scenarios, we adopt a hard-coded approach for polarity assignment. This approach is motivated by the underlying assumption in our bipolarity detection mechanism that positive and negative tokens are independently distributed. However, in the domain of code, syntax and related constraints often result in significant dependencies between nearby tokens, necessitating the use of a hard-coded strategy. Nonetheless, this approach may not ensure watermark integrity in all cases. Additionally, the variation in token counts across different code tasks poses challenges to achieving the theoretically optimal ratio of positive and

negative tokens. In future work, we aim to explore more robust methods for polarity assignment to address these limitations.

References

- Austin, J., Odena, A., Nye, M., Bosma, M., Michalewski, H., Dohan, D., Jiang, E., Cai, C., Terry, M., Le, Q., et al. Program synthesis with large language models. *arXiv preprint arXiv:2108.07732*, 2021.
- Bender, E. M., Gebru, T., McMillan-Major, A., and Shmitchell, S. On the dangers of stochastic parrots: Can language models be too big? In *Proceedings of the 2021 ACM Conference on Fairness, Accountability, and Transparency*, New York, NY, USA, 2021. Association for Computing Machinery.
- Bergman, A. S., Abercrombie, G., Spruit, S., Hovy, D., Dinan, E., Boureau, Y.-L., and Rieser, V. Guiding the release of safer E2E conversational AI through value sensitive design. In *Proceedings of the 23rd Annual Meeting of the Special Interest Group on Discourse and Dialogue*, September 2022.
- Boucher, N., Shumailov, I., Anderson, R., and Papernot, N. Bad characters: Imperceptible nlp attacks. In *2022 IEEE Symposium on Security and Privacy (SP)*, pp. 1987–2004. IEEE, 2022.
- Brassil, J. T., Low, S., Maxemchuk, N. F., and O’Gorman, L. Electronic marking and identification techniques to discourage document copying. *IEEE Journal on Selected Areas in Communications*, 13(8):1495–1504, 1995.
- Bubeck, S., Chandrasekaran, V., Eldan, R., Gehrke, J., Horvitz, E., Kamar, E., Lee, P., Lee, Y. T., Li, Y., Lundberg, S., et al. Sparks of artificial general intelligence: Early experiments with gpt-4. *arXiv preprint arXiv:2303.12712*, 2023.
- Chen, M., Tworek, J., Jun, H., Yuan, Q., Pinto, H. P. D. O., Kaplan, J., Edwards, H., Burda, Y., Joseph, N., Brockman, G., et al. Evaluating large language models trained on code. *arXiv preprint arXiv:2107.03374*, 2021.
- Christ, M., Gunn, S., and Zamir, O. Undetectable watermarks for language models. *arXiv preprint arXiv:2306.09194*, 2023a.
- Christ, M., Gunn, S., and Zamir, O. Undetectable watermarks for language models. *arXiv preprint arXiv:2306.09194*, 2023b.
- Crothers, E., Japkowicz, N., and Viktor, H. Machine generated text: A comprehensive survey of threat models and detection methods. In *Proceedings of arXiv*, arXiv, 2022. arXiv. doi: 10.48550/arXiv.2210.07321. URL <http://arxiv.org/abs/2210.07321>.
- Fellbaum, C. *WordNet: An electronic lexical database*. MIT Press, 1998.
- Fernandez, P., Chain, A., Tit, K., Chappelier, V., and Furon, T. Three bricks to consolidate watermarks for large language models. In *2023 IEEE International Workshop on Information Forensics and Security (WIFS)*, pp. 1–6. IEEE, 2023.
- Grinbaum, A. and Adomaitis, L. The ethical need for watermarks in machine-generated language. In *Proceedings of arXiv*, arXiv, 2022. arXiv. doi: 10.48550/arXiv.2209.03118. URL <http://arxiv.org/abs/2209.03118>.
- Holtzman, A., Buys, J., Du, L., Forbes, M., and Choi, Y. The curious case of neural text degeneration. *arXiv preprint arXiv:1904.09751*, 2019.
- Jawahar, G., Abdul-Mageed, M., and Lakshmanan, L. V. Automatic detection of machine generated text: A critical survey. *arXiv preprint arXiv:2011.01314*, 2020.
- Kirchenbauer, J., Geiping, J., Wen, Y., Katz, J., Miers, I., and Goldstein, T. A watermark for large language models. In *International Conference on Machine Learning*, 2023a. URL <https://api.semanticscholar.org/CorpusID:256194179>.
- Kirchenbauer, J., Geiping, J., Wen, Y., Shu, M., Saifullah, K., Kong, K., Fernando, K., Saha, A., Goldblum, M., and Goldstein, T. On the reliability of watermarks for large language models. *arXiv preprint arXiv:2306.04634*, 2023b.
- Kuditipudi, R., Thickstun, J., Hashimoto, T., and Liang, P. Robust distortion-free watermarks for language models. *arXiv preprint arXiv:2307.15593*, 2023.
- Langley, P. Crafting papers on machine learning. In Langley, P. (ed.), *Proceedings of the 17th International Conference on Machine Learning (ICML 2000)*, pp. 1207–1216, Stanford, CA, 2000. Morgan Kaufmann.
- Lee, T., Hong, S., Ahn, J., Hong, I., Lee, H., Yun, S., Shin, J., and Kim, G. Who wrote this code? watermarking for code generation. Association for Computational Linguistics, 2024. URL <https://aclanthology.org/2024.acl-long.268>.
- Li, R., Ben Allal, L., Zi, Y., Muennighoff, N., Kocetkov, D., Mou, C., Marone, M., Akiki, C., Li, J., Chim, J., et al. Starcoder: May the source be with you! *arXiv preprint arXiv:2305.06161*, 2023.

- Liu, A., Pan, L., Hu, X., Meng, S., and Wen, L. A semantic invariant robust watermark for large language models. In *The Twelfth International Conference on Learning Representations*, 2024.
- Lu, Y., Liu, A., Yu, D., Li, J., and King, I. An entropy-based text watermarking detection method. *Proceedings of the 62nd Annual Meeting of the Association for Computational Linguistics*, 2024.
- Munyer, T. J. E. and Zhong, X. Deeptextmark: Deep learning based text watermarking for detection of large language model generated text. *ArXiv*, abs/2305.05773, 2023. URL <https://api.semanticscholar.org/CorpusID:258588289>.
- OpenAI. Chatgpt: Optimizing language models for dialogue. <https://openai.com/blog/chatgpt/>, November 2022. Accessed: 2024-11-25.
- Por, L. Y., Wong, K., and Chee, K. O. Unispach: A text-based data hiding method using unicode space characters. *Journal of Systems and Software*, 85(5):1075–1082, 2012. doi: 10.1016/j.jss.2011.12.023.
- Radford, A., Kim, J. W., Xu, T., Brockman, G., McLeavey, C., and Sutskever, I. Robust speech recognition via large-scale weak supervision. In *International conference on machine learning*, pp. 28492–28518. PMLR, 2023.
- Raffel, C., Shazeer, N., Roberts, A., Lee, K., Narang, S., Matena, M., Zhou, Y., Li, W., and Liu, P. J. Exploring the limits of transfer learning with a unified text-to-text transformer. *J. Mach. Learn. Res.*, 21(1), January 2020. ISSN 1532-4435.
- Ren, J., Xu, H., Liu, Y., Cui, Y., Wang, S., Yin, D., and Tang, J. A robust semantics-based watermark for large language model against paraphrasing. In *Findings of the Association for Computational Linguistics: NAACL 2024*. Association for Computational Linguistics, 2024. doi: 10.18653/v1/2024.findings-naacl.40. URL <https://aclanthology.org/2024.findings-naacl.40>.
- Sato, R., Takezawa, Y., Bao, H., Niwa, K., and Yamada, M. Embarrassingly simple text watermarks. *arXiv preprint*, 2023.
- Topkara, U., Topkara, M., and Atallah, M. J. The hiding virtues of ambiguity: quantifiably resilient watermarking of natural language text through synonym substitutions. In *Proceedings of the 8th Workshop on Multimedia and Security*, pp. 164–174, 2006.
- Touvron, H., Lavril, T., Izacard, G., Martinet, X., Lachaux, M.-A., Lacroix, T., Rozière, B., Goyal, N., Hambro, E., Azhar, F., Rodriguez, A., Joulin, A., Grave, E., and Lample, G. Llama: Open and efficient foundation language models. *ArXiv*, abs/2302.13971, 2023. URL <https://api.semanticscholar.org/CorpusID:257219404>.
- Tu, S., Sun, Y., Bai, Y., Yu, J., Hou, L., and Li, J. Waterbench: Towards holistic evaluation of watermarks for large language models. *arXiv preprint arXiv:2311.07138*, 2023.
- Wang, L., Yang, W., Chen, D., Zhou, H., Lin, Y., Meng, F., Zhou, J., and Sun, X. Towards codable text watermarking for large language models. *arXiv preprint arXiv:2307.15992*, 2023.
- Wyllie, S., Shumailov, I., and Papernot, N. Fairness feedback loops: training on synthetic data amplifies bias. In *The 2024 ACM Conference on Fairness, Accountability, and Transparency*, pp. 2113–2147, 2024.
- Yang, X., Zhang, J., Chen, K., Zhang, W., Ma, Z., Wang, F., and Yu, N. Tracing text provenance via context-aware lexical substitution. In *Proceedings of the AAAI Conference on Artificial Intelligence*, volume 36, pp. 11613–11621, 2022.
- Yang, X., Chen, K., Zhang, W., Liu, C., Qi, Y., Zhang, J., Fang, H., and Yu, N. Watermarking text generated by black-box language models. *arXiv preprint*, 2023.
- Yoo, K., Ahn, W., and Kwak, N. Advancing beyond identification: Multi-bit watermark for large language models. In *Proceedings of the 2024 Conference of the North American Chapter of the Association for Computational Linguistics: Human Language Technologies (Volume 1: Long Papers)*, pp. 4031–4055, 2024. doi: 10.18653/v1/2024.naacl-long.224. URL <https://aclanthology.org/2024.naacl-long.224>.
- Zhang, S., Roller, S., Goyal, N., Artetxe, M., Chen, M., Chen, S., Dewan, C., Diab, M., Li, X., Lin, X. V., et al. Opt: Open pre-trained transformer language models. *arXiv preprint arXiv:2205.01068*, 2022.
- Zhao, X., Ananth, P., Li, L., and Wang, Y.-X. Provable robust watermarking for ai-generated text. *arXiv preprint arXiv:2306.17439*, 2023.

A. Preliminaries

A.1. Language model basics

Here, we introduce the fundamental concept of LLMs as well as the principles of embedding and detecting watermarks during the logits generation phase. An LLM, denoted as M , takes a prompt as input and generates subsequent tokens as its response. Specifically, let the initial prompt be x_{prompt} . At the i -th step, the input to the LLM consists of x_{prompt} and the sequence of already-generated tokens $s_{:i-1}$. Based on this input, the LLM predicts the probability distribution for the next token t_i over the vocabulary V , represented as logits l_i :

$$l_i = M(x_{\text{prompt}}, s_{:i-1}). \quad (2)$$

The next token t_i is then selected from the predicted logits l_i using techniques such as nucleus sampling, greedy decoding, or beam search. The sampling process can be expressed as:

$$t_i = \mathcal{S}(\text{softmax}(l_i)), \quad (3)$$

where \mathcal{S} denotes the specific sampling method used to choose the next token.

A.2. Watermarking during Logits Generation

KGW partitions the vocabulary into a red list (R) and a green list (G) at each token position, determined by a hash function that depends on the preceding token sequence. For the i -th token generation by the model, a bias δ is applied to the logits of tokens in G . The adjusted logit value $\tilde{l}(i)$ for a token v at position i is calculated as follows:

$$\tilde{l}(i)[v] = \begin{cases} l(i)[v] + \delta, & v \in G \\ l(i)[v], & v \in R \end{cases} \quad (4)$$

Here, $l(i)[v]$ represents the original logit value for token v at position i , and $\tilde{l}(i)[v]$ is the modified logit value after applying the watermarking bias. To detect the watermark, the algorithm classifies each token as either green or red based on the same hash function used during watermark embedding. It then calculates the green token ratio and evaluates it using the z-metric, defined as:

$$z = \frac{|s|_G - T \cdot \gamma}{\sqrt{T \cdot \gamma \cdot (1 - \gamma)}}, \quad (5)$$

Below, we discuss the concept of spike entropy, the theoretical lower bound for the number of green tokens embedded with watermarks, and the factors influencing perplexity.

Spike Entropy. Spike Entropy as defined by [Kirchenbauer et al. \(2023a\)](#) is used for measuring how spread out a distribution is. Given a token probability vector \mathbf{p} and a scalar m , the spike entropy of \mathbf{p} with modulus m is defined as:

$$S(\mathbf{p}, m) = \sum_k p_k \frac{1}{1 + mp_k}. \quad (6)$$

Theoretical Lower Bound for Green Tokens. We first introduce an important lemma from [Kirchenbauer et al. \(2023a\)](#):

Lemma A.1. *Suppose a language model produces a raw (pre-watermark) probability vector $p \in (0, 1)^N$. Randomly partition \mathbf{p} into a green list of size γN and a red list of size $(1 - \gamma)N$. Form the corresponding watermarked distribution by boosting the green list logits by δ . Define $\alpha = \exp(\delta)$. The probability that the token is sampled from the green list is at least:*

$$P[k \in G] \geq \frac{\gamma \alpha}{1 + (\alpha - 1)\gamma} S(p, \frac{(1 - \gamma)(\alpha - 1)}{1 + (\alpha - 1)\gamma}).$$

Therefore, the expected number of green list tokens in a sequence can be expressed as:

$$\mathbb{E}|s|_G \geq \frac{\gamma\alpha T}{1 + (\alpha - 1)\gamma} S^*, \quad (7)$$

where S^* represents the average spike entropy of the sequence, and $\alpha = \exp(\delta)$.

Theoretical Bound on Perplexity of Watermarked Text. We introduce an important lemma from Kirchenbauer et al. (2023a), which provides the theoretical value of the perplexity of watermarked text:

Lemma A.2. *Consider a sequence $s(i)$ where $-N_p < i < T$. Suppose the non-watermarked language model generates a probability vector $p^{(T)}$ for the token at position T . The watermarked model predicts the token at position T using a modified probability vector $\hat{p}^{(T)}$. The expected perplexity of the T -th token, taking into account the randomness of the red list partition, is given by*

$$\mathbb{E}_{W,B} \sum_k \hat{p}_k^{(T)} \ln(p_k^{(T)}) \leq (1 + (\alpha - 1)\gamma) P^*,$$

where $P^* = \sum_k p_k^{(T)} \ln(p_k^{(T)})$ represents the perplexity of the original model.

This tells us that the perplexity of the watermarked text is solely dependent on γ and the additional watermark bias δ .

A.3. Example of Inaccurate Non-Watermarked Text Estimations on Detection

Figure 7 illustrates a detection failure caused by inaccurate estimation of green token counts in non-watermarked text, assuming a z -value threshold of 4.0 for watermark detection. KGW assumes that the green token count in non-watermarked text equals γT , which is not always accurate. In this example, the green token count in human-written text is 79, while the spike entropy values for human-written and watermarked text are 0.799 and 0.795, respectively. According to Equation 7, the theoretical lower bound for green tokens in non-watermarked text is 79.85. Adjusting the expected green token count to 79 or 79.85 enables correct detection of the watermarked text.

B. Application of BiMarker in SWEET and EWD

B.1. Applying BiMarker to SWEET

SWEET builds upon KGW and is designed for code generation tasks. Unlike KGW, SWEET applies a bias δ to the logits of tokens in G only if their entropy exceeds a certain threshold τ . In other words, SWEET does not enforce the green-red rule on low-entropy tokens. The formula for calculating the z -value in SWEET is as follows:

$$z = \frac{|s|_G^h - \gamma T_h}{\sqrt{T_h \gamma (1 - \gamma)}}, \quad (8)$$

where $|s|_G^h$ represents the number of green tokens in s that have an entropy value H_t higher than the threshold τ , and T_h denotes the total number of tokens that have an entropy value higher than the threshold τ .

When applying the bipolar watermarking rule, we will only apply a bias δ to the logits of tokens in G for the positive pole or to the logits of tokens in R for the negative pole, provided that their entropy exceeds the threshold τ . The z -statistic for the differential detection method is calculated as follows:

$$z = \frac{|s|_{pG}^h - |s|_{nG}^h - \gamma T_p^h + (1 - \gamma) T_n^h}{\sqrt{T_h \gamma (1 - \gamma)}}, \quad (9)$$

where $|s|_{pG}^h$ and $|s|_{nG}^h$ represent the number of positive pole and negative pole green tokens in s that have an entropy value higher than the threshold τ . T_p^h and T_n^h denote the total number of tokens in s for the positive and negative poles, respectively, with an entropy value exceeding the threshold τ .

Prompt	
<p>Gary Rowett has backed Steve Bruce as the right appointment for Aston Villa but warned his city rival the club will expect promotion for the amount of money spent on transfers. The Birmingham manager raised the pressure on his opposite number ahead of Saturday's second city derby by insisting Villa owner Tony Xia will be 'disappointed' if the squad assembled fails to at least challenge the play-offs. Villa spent £50million on new players during the summer window and have a team the envy of the Championship, including the second tier's most expensive player ever in £</p>	
Real Completion	
<p>15m Jonathan Kodjia. 'If I was the person signing the cheques, I'd be a little bit disappointed if I didn't have a squad that could get them up,' said Rowett. 'You'd hope so with the amount of money spent. Birmingham head into the first league derby between the sides since 2011 placed in seventh, six points and nine places better off than Villa despite a much smaller budget. But Rowett believes Villa, with seven points from three games under Bruce, have picked the best replacement for Roberto Di Matteo. 'Yes, I think he was. I'm not going to turn around and lie about that. I think he was a fantastic choice for them and for any Championship club that needs a bit of pragmatism and a little bit of understanding about what's required for promotion, because he's done it,' said Rowett.</p>	<p>S=0.799 z=-2.906 Actually green tokens:79 Theoretical green tokens: 79.85</p>
Watermarked	
<p>'It was always going to be difficult for him, he's had a very good job at Chelsea. There's a lot of things he had to get right but as I said, it was going to be difficult for him. Saturday's clash in the city will be a chance for Bruce to show what he has learned in taking on a Villa side he twice lost to in the play-offs. 'The first thing I said to him is, "Look, I know you're a very good coach, but you're not good enough to get promoted",' said Rowett. '</p>	
<p>And he said "Yeah, I know I'm not good enough". I said "No, you're not good enough". 'Villa have been hit by injuries to midfielders Jack Grealish and John McGinn, plus winger Douglas.</p>	<p>s=0.795 z=(110-50)/sqrt(200x0.5x0.5)=1.489 ❌ z=(110-79)/sqrt(200x0.5x0.5)= 4.384 ✅ z=(110-79.85)/sqrt(200x0.5x0.5)= 4.264 ✅ Green tokens:110</p>

Figure 7. Detection Impact from Inaccurate Non-Watermarked Text Estimations with Watermarked Text (where γ is 0.5 and δ is 1.0) Generated by OPT-1.3, assuming classification as watermarked text occurs when the z -value exceeds 4.0.

B.2. Applying BiMarker to EWD

EWD is another watermark detection algorithm based on KGW. Specifically, it proposes that a token's influence during detection should be proportional to its entropy. To fully reflect this positive relationship between token entropy and detection influence, a monotonically increasing and continuous function is utilized to generate influence weights from token entropy.

The weight $W(t)$ of a token t is defined as follows:

$$W(t) = f(SE(t) - C_0), \tag{10}$$

where $SE(t)$ represents the token's entropy and C_0 is the minimal value of spike entropy, used to normalize the entropy input before computing the weight.

To calculate the z -score using the provided formula:

$$z = \frac{|s|_G^W - \gamma \sum W_i}{\sqrt{\gamma(1 - \gamma) \sum W_i^2}}. \tag{11}$$

EWD modifies only the watermark detection method, while the watermark generation algorithm remains the same as KGW.

Therefore, when applying the bipolar watermark, the process as shown in Algorithm 1. During detection, we utilize the differential detection algorithm:

$$z = \frac{|s|_{pG}^W - |s|_{nG}^W - \gamma \sum_{i \in p} W_i + (1 - \gamma) \sum_{i \in n} W_i}{\sqrt{\gamma(1 - \gamma) \sum W_i^2}}, \quad (12)$$

where $|s|_{pG}^W$ and $|s|_{nG}^W$ represent the weighted sums of green tokens in the positive and negative poles, respectively. Additionally, $\sum_{i \in p} W_i$ and $\sum_{i \in n} W_i$ denote the weighted sums of all tokens in the positive and negative poles, respectively.

C. Proofs of Theorems 3.1 and 3.2

C.1. Proof of Theorem 3.1

In the KGW framework, we can derive a lower bound for the number of green list tokens in s by summing the results of lemma A.1. The lower bound of the expected number of green list tokens is given by: $\mathbb{E}(|s|_G) \geq \frac{\gamma \alpha T}{1 + (\alpha - 1)\gamma} S^*$, where S^* represents the average spike entropy of the generated sequence. By applying the definition of the z -score from Equation 5, we obtain a lower bound for the z -score:

$$z_k \geq \frac{\frac{\gamma \alpha T}{1 + (\alpha - 1)\gamma} S^* - \gamma T}{\sqrt{T\gamma(1 - \gamma)}}, \quad (13)$$

where $\alpha = \exp(\delta)$.

When using bipolar watermarking, we assume that the processes for positive and negative polarities are independent. The number of green tokens in the positive polarity, according to (7), is at least: $\frac{\gamma \alpha T_p}{1 + (\alpha - 1)\gamma} S^*$. Similarly, we assume that the entropy of the negative polarity is maximized, meaning that each token follows a uniform probability distribution. Under this condition, the expected number of green tokens in the negative polarity reaches its maximum, given by: $\frac{\gamma T_n}{1 + (\alpha - 1)\gamma}$, the expected difference between the two polarities of green tokens is given by:

$$\mathbb{E}|s_d| \geq \frac{\alpha \gamma T_p}{1 + (\alpha - 1)\gamma} S_p^* - \frac{\gamma T_n}{1 + (\alpha - 1)\gamma}, \quad (14)$$

where S_p^* is the average spike entropy of the positive polarity sequence. We substitute this into the calculation formula for the z -score (9) to obtain:

$$z_d \geq \frac{\frac{\alpha \gamma T_p}{1 + (\alpha - 1)\gamma} S_p^* - \frac{\gamma T_n}{1 + (\alpha - 1)\gamma} - \gamma T_p + (1 - \gamma) T_n}{\sqrt{T\gamma(1 - \gamma)}}. \quad (15)$$

We denote the right-hand sides of (13) and (15) as $\mathcal{B}(|z|_k)$ and $\mathcal{B}(|z|_d)$, respectively. The difference $\mathcal{B}(|z|_d) - \mathcal{B}(|z|_k)$ is given by:

$$\mathcal{B}(|z|_d) - \mathcal{B}(|z|_k) = \frac{\frac{\alpha \gamma T_p}{1 + (\alpha - 1)\gamma} S_p^* - \frac{\gamma T_n}{1 + (\alpha - 1)\gamma} - \gamma T_p + (1 - \gamma) T_n}{\sqrt{T\gamma(1 - \gamma)}} - \frac{\frac{\gamma \alpha T}{1 + (\alpha - 1)\gamma} S^* - \gamma T}{\sqrt{T\gamma(1 - \gamma)}}. \quad (16)$$

We assume that S^* is equal to S_p^* . By substituting this assumption into Equation (16), we can simplify it to:

$$\begin{aligned} \mathcal{B}(|z|_d) - \mathcal{B}(|z|_k) &= \frac{-\frac{\gamma \alpha T_n}{1 + (\alpha - 1)\gamma} S^* - \frac{\gamma T_n}{1 + (\alpha - 1)\gamma} + T_n}{\sqrt{T\gamma(1 - \gamma)}} \\ &\geq \frac{-\frac{\gamma \alpha T_n}{1 + (\alpha - 1)\gamma} - \frac{\gamma T_n}{1 + (\alpha - 1)\gamma} + T_n}{\sqrt{T\gamma(1 - \gamma)}} = 0, \end{aligned} \quad (17)$$

In the last step, we utilized the fact that the value of cross-entropy cannot exceed 1. Therefore, we have successfully proven Theorem 3.1.

Discussion on the Effectiveness of Applying BiMarker to EWD We first introduce the statistical weight and expectation of EWD. Following the original paper (Lu et al., 2024), for analysis purposes, we adopt a linear weight function for each token k :

$$W(k) = SE(k) - C_0,$$

where C_0 is a constant. Based on Lemma A.1, the average of the sum of weights for green tokens can be obtained as: $\sum_k P[k \in G] \cdot W(k)$. By applying the definition of the z -score from Equation 11, we obtain a lower bound for the z -score:

$$z_e \geq \frac{\frac{\gamma\alpha T}{1+(\alpha-1)\gamma} SW^* - \gamma \sum W_i}{\sqrt{\gamma(1-\gamma) \sum W_i^2}}, \quad (18)$$

where SW^* represents the mean of the product of entropy and weight.

Following a similar logic to Equation (14) and based on Equation (9), the minimum expected value of the detection z -score, when applying bipolar watermarking and differential detection algorithms, can be derived as:

$$z_d \geq \frac{\frac{\gamma\alpha T_p}{1+(\alpha-1)\gamma} SW_p^* - \frac{\gamma T_p}{1+(\alpha-1)\gamma} SW_n^* - \gamma \sum_{i \in p} W_i + (1-\gamma) \sum_{i \in n} W_i}{\sqrt{\gamma(1-\gamma) \sum W_i^2}}, \quad (19)$$

where SW_p^* and SW_n^* denote the mean of the product of entropy and weight for the tokens in the positive and negative poles, respectively.

We denote the right-hand sides of (18) and (19) as $\mathcal{B}(|z|_e)$ and $\mathcal{B}(|z|_d)$, respectively. Assuming the mean of the product of entropy and weight for positive and negative samples is identical, the difference $\mathcal{B}(|z|_d) - \mathcal{B}(|z|_e)$ is expressed as:

$$\mathcal{B}(|z|_d) - \mathcal{B}(|z|_e) = \frac{-\frac{\gamma\alpha T_n}{1+(\alpha-1)\gamma} SW^* - \frac{\gamma T_n}{1+(\alpha-1)\gamma} W_n^* - \gamma \sum_{i \in p} W_i + (1-\gamma) \sum_{i \in n} W_i + \gamma \sum W_i}{\sqrt{\gamma(1-\gamma) \sum W_i^2}}.$$

Due to the maximum value of spiked entropy being less than 1, we simplify the numerator and obtain:

$$\mathcal{B}(|z|_d) - \mathcal{B}(|z|_e) \geq \frac{T_n W^* - \sum_{i \in n} W_i}{\sqrt{\gamma(1-\gamma) \sum W_i^2}} = 0.$$

C.2. Proof of Theorem 3.2

We assume that when the z value exceeds the threshold $z_{\text{threshold}}$, the text being tested is classified as watermarked. We define $t = z_{\text{threshold}} \sqrt{T\gamma(1-\gamma)}$. Thus, the false positive rate when using the KGW detection method for non-watermarked text can be expressed as:

$$F_{\text{KGW}} = P(x > \mu_T + t | \text{non-watermarked}) = \int_{\mu_T + t}^{+\infty} \frac{1}{\sqrt{2\pi}\sigma_T} e^{-\frac{(x-\mu_T)^2}{2\sigma_T^2}} dx = 1 - \Phi\left(\frac{t}{\sigma_T}\right). \quad (20)$$

where x represents the number of green tokens in the non-watermarked text, Φ represents the cumulative distribution function of the standard normal distribution.

Under the differential method, if y and x are the numbers of green tokens in the positive and negative polarities, respectively, and $y - x > t$, the text is classified as watermarked. The false positive rate can then be expressed as:

$$F_{\text{Diff}} = P(y - x > t | \text{non-watermarked}) = \int_{-\infty}^{+\infty} \int_{x+t}^{+\infty} f(x)f(y) dy dx = \int_{-\infty}^{+\infty} 1 - \Phi\left(\frac{x+t-\mu_{T_n}}{\sigma_{T_p}}\right) dx \quad (21)$$

where $f(x)$ and $f(y)$ are the Gaussian probability density functions for the negative and positive polarities, respectively:

$$f(x) = \frac{1}{\sqrt{2\pi}\sigma_{T_n}} e^{-\frac{(x-\mu_{T_n})^2}{2\sigma_{T_n}^2}}, \quad f(y) = \frac{1}{\sqrt{2\pi}\sigma_{T_p}} e^{-\frac{(y-\mu_{T_p})^2}{2\sigma_{T_p}^2}}.$$

Continuing to simplify (21), since the Φ function is monotonically increasing and $x - \gamma T_n > 0$, along with $\sigma_{T_p} \leq \sigma_T$, we can derive:

$$F_{\text{Diff}} \leq \int_{-\infty}^{+\infty} 1 - \Phi\left(\frac{t}{\sigma_T}\right) dx = 1 - \Phi\left(\frac{t}{\sigma_T}\right) = F_{KGW}. \quad (22)$$

Thus, Theorem 3.2 is proven.

Discussion on the Effectiveness of Applying BiMarker to EWD. Our proof process is highly similar to that of KGW. The key difference lies in $t = z_{\text{threshold}} \sqrt{\gamma(1-\gamma)} \sum W_i^2$, and the Gaussian distribution represents the distribution of green token weights rather than the distribution of the number of green tokens.

D. Experimental Details

D.1. Hyper-parameters

Hyper-parameters. For high-entropy tasks, multinomial sampling employs a fixed sampling temperature of 0.7. In contrast, beam-search sampling utilizes 8 beams, with a *no_repeated_ngrams* constraint set to 16 to mitigate excessive text repetition. For low-entropy tasks, specifically code generation, we adopt top-p sampling (Holtzman et al., 2019) with $p = 0.95$ and a lower temperature of 0.2. When using SWEET for watermark embedding and detection, we set the entropy threshold to 0.695, consistent with (Lee et al., 2024; Lu et al., 2024), and exclude all tokens below this threshold during both processes.

D.2. ROC Curves

Figure 8 presents the ROC curves for KGW and BiMarker with γ set to 0.25 and 0.5, and δ set to [0.5, 0.75, 1.0, 1.5, 2, 2.5], using polynomial sampling and beam search with a beam size of 8. The perplexity (PPL) of the generated completions is computed using a larger oracle language model (OPT-2.7B). Both standard coordinate axes and logarithmic axes are plotted. The results demonstrate that BiMarker is more effective at distinguishing between watermarked and non-watermarked text, particularly at low false positive rates and low watermark strengths.

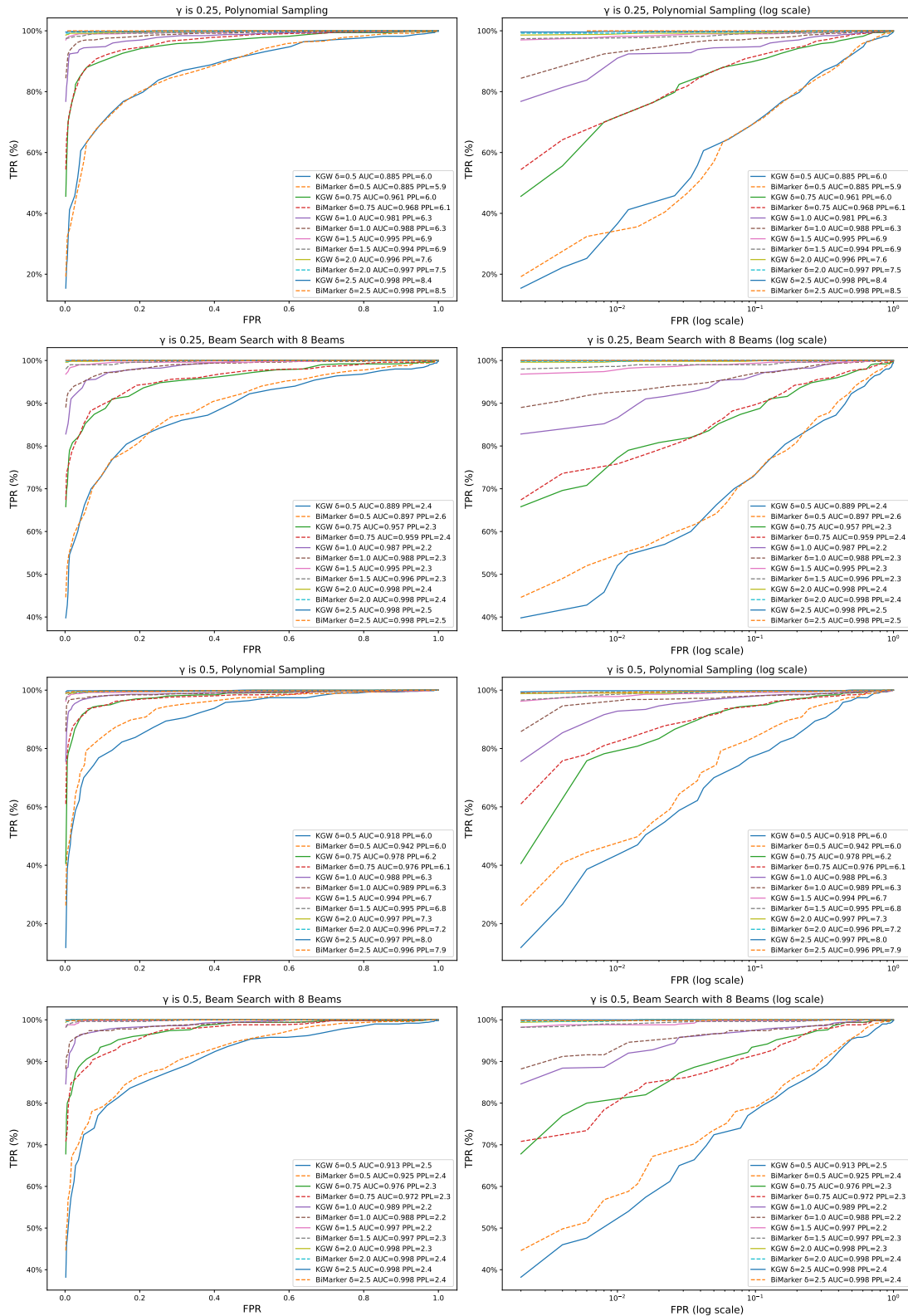


Figure 8. ROC Curves with AUC Values and PPL Under Different Hyperparameter Settings (Normal and Semilog Axes).